ELSEVIER

European Journal of Mechanics B/Fluids 21 (2002) 237–246

EUROPEAN JOURNAL OF MECHANICS B/FLUIDS

Unstable waves at the interface of a diamagnetic liquid column contained in a magnetic fluid

Jianqiang Mai [a,*], Ryuichiro Yamane [b], Wolf-Gerrit Früh [a], Shuzo Oshima [c], Atsushi Ando [d]

[a] *Department of Mechanical & Chemical Engineering, Heriot-Watt University, Edinburgh, EH14 4 AS, UK*
[b] *Department of Mechanical Engineering, Kokushikan University, 4-28-1 Setagaya, Setagaya-ku, Tokyo 154-8515, Japan*
[c] *Department of Mechanical Engineering and Science, Tokyo Institute of Technology, 2-12-1 O-okayama, Meguro-ku, Tokyo 152-8552, Japan*
[d] *Toyota Machine Works, LTD, Aichi, Japan*

Received 1 December 2000; received in revised form 11 June 2001; accepted 13 September 2001

Abstract

A magnetically held pipeless fluid transporting system is a potentially useful noncontact technique in science and technology. Keeping a stable interface between the diamagnetic liquid column and the surrounding magnetic fluid is essential. The present study gives an experimental study on the unstable interfacial wave leading to discontinuity of a liquid column maintained in a magnetic fluid by a non-uniform magnetic field. The experiments were carried out by setting two magnetic north poles in opposite position to produce the magnetic field, using water to form the diamagnetic liquid column, and a diluted kerosene-base magnetic fluid as the surrounding fluid. Unstable interfacial waves were measured. It was found that the magnetic pressure acting on the interface can stabilise the interface. The experimental results agree well with the theoretical stability condition derived from a two-fluids model.

Keywords: Ferrohydrodynamics; Magnetic fluid; Oscillatory flow; Stability; Levitation

1. Introduction

A noncontact technique is a technique used to hold or manipulate liquid materials in the absence of a container. It is increasingly used in containerless solidification [1], crystal growth [2], material property measurement and material processing [3], medical industry [4], microstructure control of materials [5] and biological applications [6], where materials must be manipulated, heated, or cooled without contact between the material and container walls. Many levitation methods have been developed so far. The material is usually levitated by magnetic levitation [7–9], electromagnetic levitation [10,11], electrostatic levitation [3,12], acoustic levitation [13,14], drop tube [15], aerodynamic levitation [16], laser levitation [17], or a combination of theses methods.

Traditionally, the use of magnetic forces was limited to magnetic materials such as iron though diamagnetism was discovered by Michael Faraday in as early as 1846. In recent years, accompanying the development of superconductor technology, materials which do not react to a common magnetic field also show, in the presence of a strong magnetic field, magnetic forces of the same order as gravity [7,18,19]. By using this magnetic force, diamagnetic materials and paramagnetic materials can be levitated in

* Correspondence and reprints.
E-mail address: jianqiang.mai@hw.ac.uk (J. Mai).

0997-7546/02/$ – see front matter
PII: S0997-7546(01)01168-2

Nomenclature

d	inlet diameter of the water column
t	time
r_0	radius of the undisturbed column
H_a	magnetic field at the interface
k	wave number
k_z	wave number in axial direction of the levitated liquid column
η_1	amplitude of the interfacial wave at $t = 0$
χ_α	magnetic susceptibilities
μ_0	the permeability of free space, $\mu_0 = 4\pi \times 10^{-7}$ Tm A^{-1}
ρ_α	density of fluids
σ	the interfacial tension coefficient
ω	angular frequency of the interfacial wave
Subscript α	indicates the undisturbed interface
$\alpha = 1$	indicates the inner diamagnetic fluid
$\alpha = 2$	indicates the surrounding magnetic fluid
Superscript $*$	identifies dimensionless quantities

an earth-based laboratory and a pipeless fluid transporting system can be built. Since most fluids are diamagnetic and magnetic levitation has many unique advantages [20], the development of a magnetic levitation technique for the levitation of diamagnetic and paramagnetic materials is of wide relevance both to science and engineering.

By placing two magnetic north poles face to face each other, a non-uniform magnetic field, which is weakest at the centre and is gradually stronger in radial direction, can be produced. When the magnetic field is strong enough, a diamagnetic fluid can stay stably at the centre of the magnetic field just like in a container [21–23]. If the opposite faces of the magnetic poles are infinitely long, the centre of the magnetic field is a line. In such a field, the magnetic forces will push the levitated fluid to the centreline forming a column along the centreline like in a virtual pipe without solid walls. Because of this phenomenon, the magnetic field is called a magnetic pipe in our paper. To produce a magnetic pipe in air or other gases, strong magnets are required. With the help of a magnetic fluid as a surrounding fluid a large part of the gravity of the levitated non-magnetic liquid can be balanced by the buoyancy. Only a small part of the gravity force needs to be balanced by the magnetic force that can thus be produced in a far weaker magnetic field, and a magnetic pipe can be created easily. It is then possible to study the hydrodynamic properties of the levitated diamagnetic fluid, and one might build eventually magnetic pipes, tanks, valves and pumps to form a containerless flow system. Such a system could be useful in many fields, such as chemical reactions, materials processing and the medical industry where contacting with other materials must be avoided.

As the magnetic pipe is formed not by solid walls but by a magnetic field, the liquid column in the magnetic pipe can be deformed or displaced from the equilibrium position. A disturbance can change not only the flow field and pressure field but also the shape of the fluid in the magnetic pipe. Under certain conditions, the liquid column is not stable and any disturbance will break the column up into separated drops. As a special case when the magnetic pipe is in vertical direction or the gravity is in axial direction of the fluid column, the present paper studies the instability of the liquid column maintained in a magnetic field by observing the unstable waves experimentally.

2. Theoretical results

In Mai et al. [22,23], the stability condition, flow field and linear wave in a liquid column maintained in a magnetic fluid by a magnetic field was discussed in details using a linear wave theory. Stable waves were measured in experiments, which showed quite good agreement with the theoretical result. It was found that the stability of the levitated liquid column is governed by the mode 0 stability. For mode 0 oscillations which dominate the stability of the levitated liquid column, it is obtained from reference [23] by setting $\nu = 0$ that the response angular frequency of the liquid column is given by

$$\omega^{*2} = \frac{(k^{*2} - 1) + r_0 f'(r_0) f(r_0) N_{\mathrm{BO}}}{-\kappa C_{21}(K_0(k^*)/K_0'(k^*)) + (1 - \kappa C_{11})(I_0(k^*)/I_0'(k^*))} \cdot k^*, \tag{1}$$

where $I_0(k^*)$ is the modified Bessel function of the first kind of order 0 and $K_0(k^*)$ is the modified Bessel function of the second kind of order 0. The constants C_{21} and C_{11} are constants determined by boundary conditions. κ is the density ratio

of the magnetic fluid to the diamagnetic fluid, $f(r)$ is the magnetic field function, and N_{BO} is the magnetic Bond number as defined given by

$$N_{\mathrm{BO}} = \mu_0(\chi_2 - \chi_1)H_a^2 r_0/\sigma. \tag{2}$$

The non-dimensionalisation has used the radius of the stable fluid column, r_0, the density of the diamagnetic fluid density, ρ_1, and the interfacial tension, σ. Then, the wave number is non-dimensionalised by $k^* = kr_0$ and the frequency by $\omega^{*2} = \rho_1 r_0^3 \omega^2/\sigma$.

The angular velocity is a pure imaginary number corresponding to the amplification of a disturbance when the disturbance wave number fulfils:

$$k^{*2} < 1 - r_0 f'(r_0) f(r_0) N_{\mathrm{BO}}. \tag{3}$$

When the right-hand side of the above inequality is equal to or smaller than 0, no disturbance can fulfil inequality (3), and the liquid column is always stable. When the right-hand side of the above inequality is larger than 0, the column is unstable because white noise disturbances always exist. As $f(r) > 0$ and $f'(r) > 0$ in a magnetic pipe, the increase in the gradient of the magnetic field can stabilise the liquid column in it. When the magnetic field is formed by s pairs of very long uniform magnetic north poles, its r-, φ- and z-direction components are:

$$H_r = H_a\left(\frac{r}{r_0}\right)^{2s-1}\cos(2s\varphi), \qquad H_\varphi = -H_a\left(\frac{r}{r_0}\right)^{2s-1}\sin(2s\varphi), \qquad H_z = 0, \tag{4}$$

and

$$H = \sqrt{H_r^2 + H_\varphi^2} = H_a f(r) = H_a\left(\frac{r}{r_0}\right)^{2s-1}, \tag{5}$$

where H is the mode of the magnetic field which dominate the magnetic pressure acting on the interface, r and φ are coordinates in the cylindrical coordinate system. In the experiments where one pair of magnets was used, $s = 1$, and the corresponding magnetic field function is $f(r) = r/r_0$, which will be used in the following of the paper without further indication.

Letting $\omega^* = -\mathrm{i}\gamma$ where γ is a positive real number, the shape of the interface takes the following form

$$\eta = \eta_1 \mathrm{e}^{\gamma t - \mathrm{i}kz}, \tag{6}$$

which suggests that the amplitude of the interfacial wave grows exponentially. Thus the wave with the largest γ will be the first to be observable in an experiment. Since, from Eq. (1), a maximum for γ implies a minimum for ω^{*2}, the most unstable wave can be found by minimising Eq. (1). There is a unique minimum of ω^{*2} for each magnetic Bond number, shown in Fig. 1. Figure 2 shows the critical wavenumber k^*, corresponding to the minimum value of ω^{*2}, as a function of the magnetic Bond number. When the magnetic Bond number is greater than 1, the critical wavenumber is always 0.

Assuming the unstable wave can be seen when the amplitude of the wave is A_m, then it follows from Eq. (6) that a disturbance can be seen after a time $t = \ln(A_m/\eta_1)/\gamma$ or a distance, l, from the origin of the magnetic pipe. At high fluid velocities, v, the distance l increases linearly with v, because $r_0 \approx d/2$ and, with it, γ are constants. At low fluid velocities, γ increases because

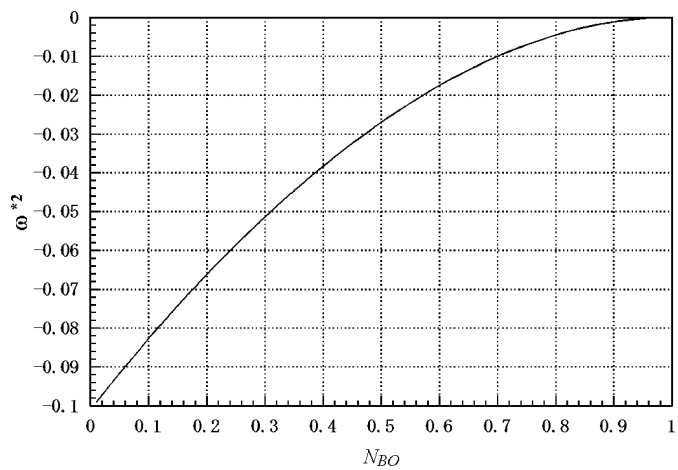

Fig. 1. Minimum of ω^{*2} as a function of the magnetic Bond number N_{BO} ($\kappa = 0.78$, $R/r_0 = 3.6$).

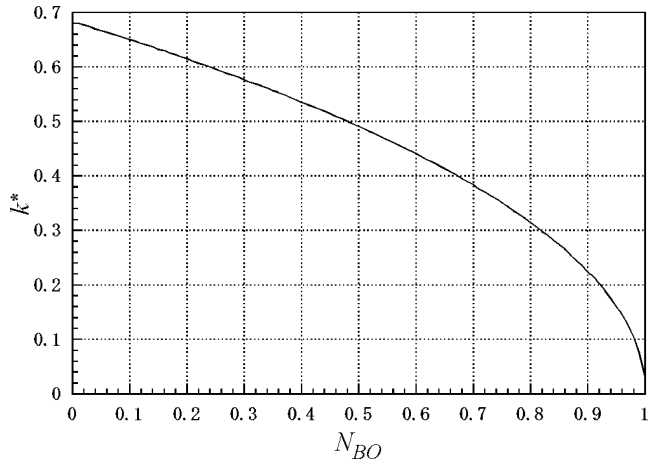

Fig. 2. Critical wavenumber k^* as a function of the magnetic Bond number, N_{BO} ($\kappa = 0.78$, $R/r_0 = 3.6$).

r_0 decreases with decreasing v due to the effect of interfacial tension and the instability becomes absolute rather than convective. Thus, there exists a velocity, v_0, below which the fluid column breaks up within a fraction of the unstable wavelength. Assuming a constant growth rate above v_0 and an immediate finite-amplitude disturbance below v_0, the length l between the outlet and the point where the unstable wave can be seen, can be written as

$$l = (v - v_0)\ln(A_m/\eta_1)/\gamma. \tag{7}$$

This length, l, can be regarded as the maximum length for which a fluid column in a magnetic pipe is stable enough for practical use when the magnetic Bond number is smaller than 1. For convenience, an amplification factor, $n = \ln(A_m/\eta_1)$, is defined.

Equation (2) shows that the magnetic Bond number, N_{BO}, can be reduced to less than 1 by reducing the radius of the inner liquid column. When the surrounding fluid is a magnetic fluid and the inner fluid is a diamagnetic one and if $N_{\mathrm{BO}} \in (0, 1)$ then a range of wave number $k^* \in (0, (2\pi r_0)/\sqrt{1 - N_{\mathrm{BO}}})$ exists, in which the inner diamagnetic liquid column is unstable.

The present experimental study will use this principle to find the wavelength at which the unstable wave is observed and what length of a magnetic pipe, l, can be supported stably for a range of average velocities of the liquid column when the magnetic Bond number N_{BO} is smaller than 1.

3. Experimental devices and method

Figure 3 shows a schematic of the experimental devices. The north poles of two magnets were set face to face forming a gap in vertical position. The size of a magnet was 200 mm × 20 mm × 20 mm. The magnetic flux density of the magnet was 0.4 T at its surface and the gap between the magnets was adjustable. An acrylic box, outer size 400 mm × 45 mm × 16 mm, inner size 394 mm × 39 mm × 10 mm, was fixed between the magnets. A water tank above the magnets was connected with the acrylic box through a flexible pipe in which a valve controlled the flow rate. A small high precision flow meter, Model XFS-1204 by Mitsuba Corporation, was used to measure the volume flow rate. Under the acrylic box, a flexible outlet pipe with a valve connected the acrylic box with a downstream tank. A high power light behind the acrylic box produced a beam strong enough to penetrate the magnetic fluid. A video camera was used to record the flow from the front of the box.

During an experiment, water flows into the acrylic box from the upper inlet and out through the lower outlet. The acrylic box is filled with a diluted kerosene-base magnetic fluid before water flows in. Because the density of water is higher than that of the magnetic fluid, the upper part of the acrylic box or the test section is always filled with the magnetic fluid, even allowing part of the magnetic fluid to flow out with water during the experiment.

To observe the inner flow, the magnetic fluid had to be diluted with kerosene. In our experiments, the maximum concentration was about 1.2 Vol% of ferrofluid in kerosene. The undiluted magnetic fluid was the HC-50 magnetic fluid (Taiho Industry Corporation, Japan) with kinematic viscosity $0.13 \times 10^{-6}\ \mathrm{m^2\,s^{-1}}$, density $1425.0\ \mathrm{kg\,m^{-3}}$, surface tension $0.0245\ \mathrm{N\,m^{-1}}$, and magnetic susceptibility 0.7. The physical properties of the diluted magnetic fluids are listed in Table 1. The gaps between the magnets were 16, 20 and 24 mm, respectively, and Fig. 4 shows the measured magnetic field for the 16 mm gap.

The inlet diameter was either 1.7 or 2.2 mm but the actual diameter of the stable water column in the tank could not be measured, as is apparent in Fig. 5 of a typical experimental result. The diameter of the water jet is treated to be approximately equal to the inlet diameter for the following reason. Because the magnetic Bond number, which compares the magnetic force

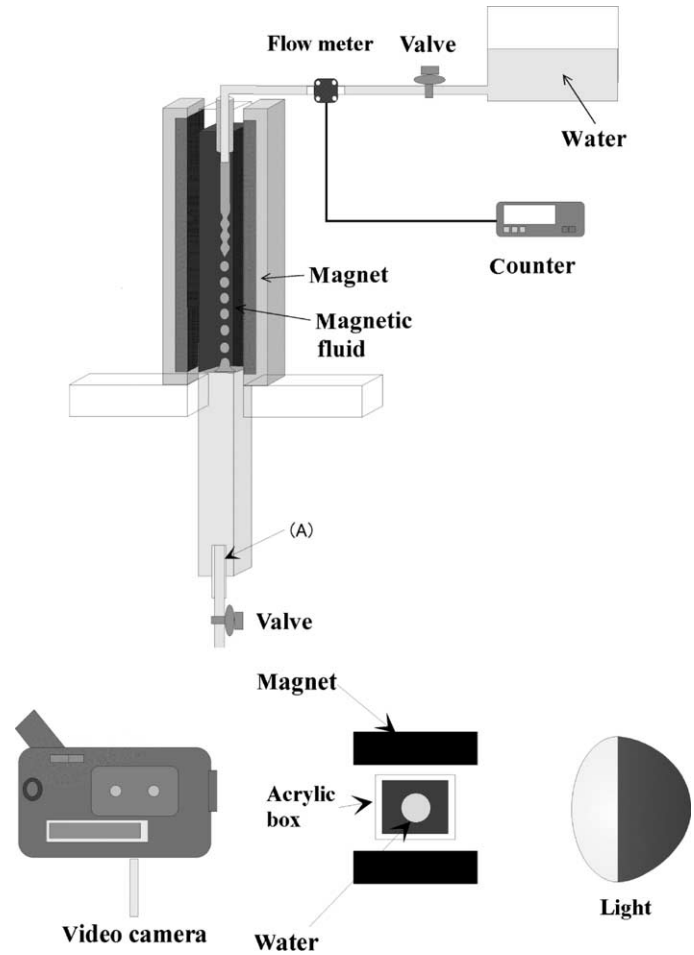

Fig. 3. Schematic of the experimental devices.

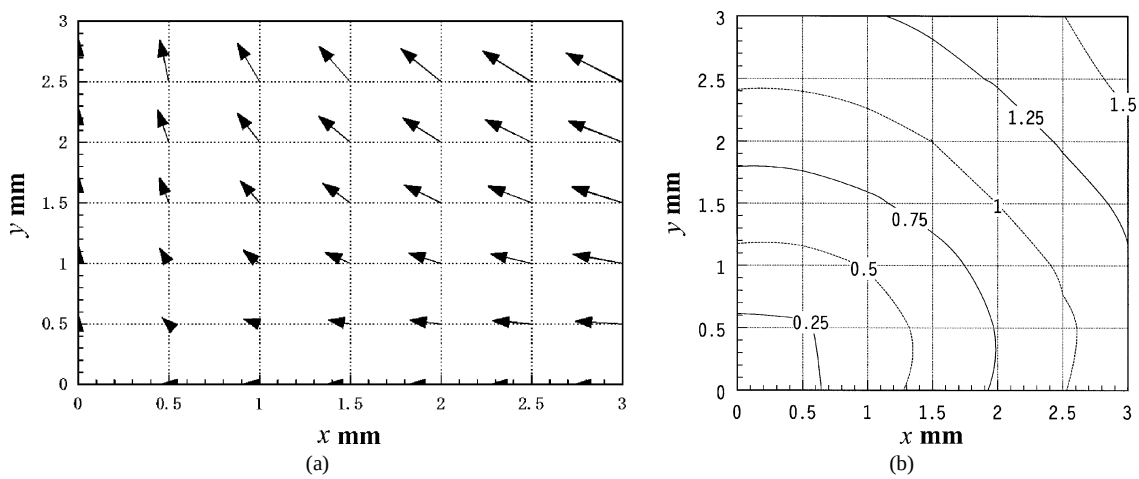

Fig. 4. Measured magnetic induction field in air (gap = 16 mm, $\times 10^3$ G): (a) vector map; (b) equivalue map.

Table 1
Physical properties of the magnetic fluids

Concentration (%)	Density $kg\,m^{-3}$	Interfacial tension $(mN\,m^{-1})$
0.5	779	45.0
0.75	780	43.5
1.0	781	40.0

to the interfacial tension, is always less than 0.2, the magnetic force is much smaller than the interfacial tension. The magnetic force may act to deform the cross-section of the water column but the stronger interfacial tension will maintain a circular cross-section. Consequently, the deformation of the cross-section may be omitted.

To perform an experiment, the acrylic box was filled first with the magnetic fluid while the valves were closed. Second, the upper valve was opened, and then very slowly the lower valve until the part of the water column near the inlet was stable and the lower part unstable. The video camera recorded the whole process from the beginning, and the image was subsequently analysed on a PC. To avoid unnecessary heating of the magnetic fluid, the light was only switched on when the camera was working.

4. Experimental results

Figure 5 is a typical image from the experiment. The permanent magnets that are held in two brass holders are indicated in the picture. The white drops are areas of large water volumes in the water column while the black area around the white drops is the magnetic fluid. Above the visible white drops, the water column is stable. A ruler is fixed on one magnet holder to give a scale for the measurement of the wavelength. The white strip at the right of the water drops is a wall of the transparent container. The unstable wavelength is the distance between two white drops when the separation can be seen. At the lower part of the acrylic box, the water drops pile up, forming a cone of water. The height of the cone becomes shorter with the increase in the concentration of the magnetic fluid.

Figures 6–8 are results for the stable length, l, of the water column before the interfacial waves have grown to a visible amplitude. The three figures refer to three different concentrations of the magnetic liquid, 0.5%, 0.75%, and 1.0%, respectively. The experimental conditions and the results are summarised in Table 2. The vertical axis is the distance l between the inlet of the inner surface of the acrylic box and the point where the water column begins to separate. The horizontal axis is the average water velocity, v, as calculated from the measured volume flow rate and the inlet diameter. The concentrations of the magnetic fluid in the three figures are 0.5%, 0.75% and 1.0%, respectively, so that the magnetic pressure acting on the interface increases from Fig. 6 to Fig. 8. In each figure, the measurements originate from three values of the magnetic field strength obtained by altering the gap between the magnets, which are identified by different symbols in the respective figures. Superimposed on

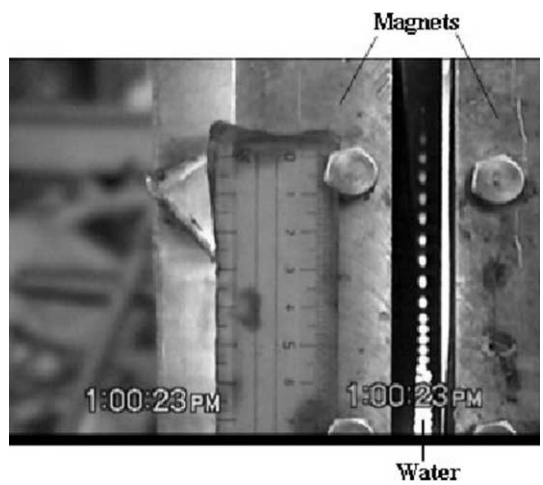

Fig. 5. A typical picture of the unstable wave.

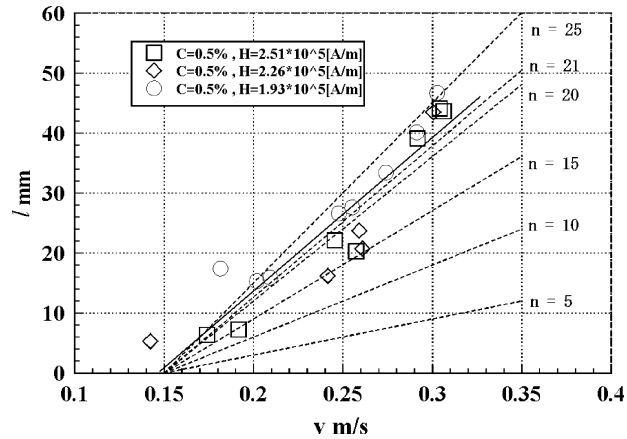

Fig. 6. Distance, l, between the inlet and the point where the column breaks for a magnetic fluid concentration of $C = 0.5\%$.

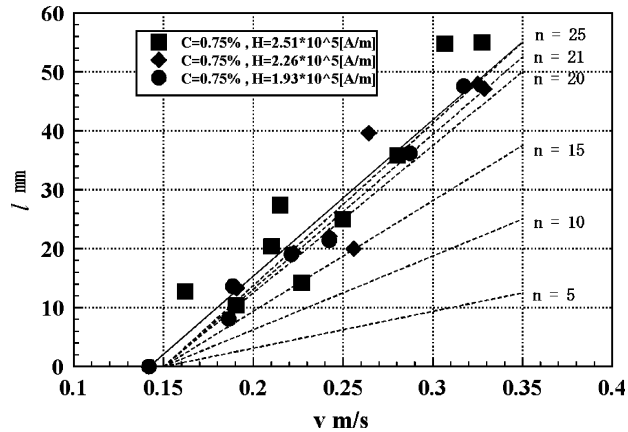

Fig. 7. Distance, l, between the inlet and the point where the column breaks for a magnetic fluid concentration of $C = 0.75\%$.

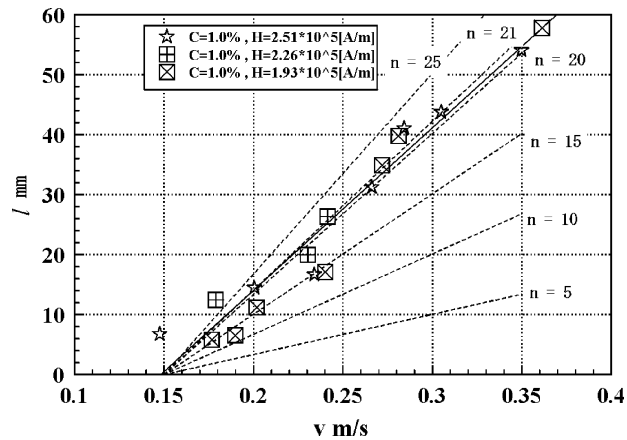

Fig. 8. Distance, l, between the inlet and the point where the column breaks for a magnetic fluid concentration of $C = 1.0\%$.

Table 2
Summary of the experiments to determine the growth rate and stable length of the liquid column. The regression straight line is $l = m(v - v_0)$

Conc. (%)	H ($\times 10^5$ A m^{-1})	N_{BO} [±20%]	v_0 (m s^{-1})	m (s)	γ (s^{-1})	$m^*\gamma$	l_{max} (mm)
0.5	1.93	0.031	0.146	0.256	83.80	21	45
	2.26	0.040	±0.024	±0.024	83.13	21	±2
	2.51	0.045			82.72	21	
0.75	1.93	0.048	0.145	0.271	81.09	22	50
	2.26	0.061	±0.019	±0.021	80.05	22	±3
	2.51	0.070			79.32	22	
1.0	1.93	0.070	0.150	0.272	76.06	21	57
	2.26	0.089	±0.016	±0.017	74.60	20	±2
	2.51	0.101			73.70	20	
Combined results			0.147	0.267			
			±0.011	±0.012			

the measurements are a linear best fit (the solid line) and a range of theoretical predictions (dashed lines) using the growth factor γ from Eq. (1) in the expression for the stable length, Eq. (7), using a selection of amplification factors, $n = \ln(A_m/\eta_1)$. The growth factor was calculated in all cases for the intermediate magnetic field of $H = 2.22$ A m^{-1}. The slope of the lines represents the ratio of the amplification factor to the growth rate, while the intercept with the v-axis identifies the critical velocity v_0, below which the liquid column breaks up immediately after entering the magnetic liquid.

All three figures show very similar results. The liquid column shows a stable region only above a finite velocity, and then the stable length increases with the liquid velocity. Furthermore, inspection by eye confirms the supposition that the stable length would increase linearly with the velocity, which was used for the formulation of Eq. (7). Comparing the results for linear regression analyses for the three graphs, listed in Table 2, reveals that no systematic trend for the minimum velocity can be detected within the experimental uncertainty. While a small trend in the slope of the regression lines, i.e. in the amplification of disturbances, is present, the changes are too small to be statistically significant. Evidence from the calculation of the growth rate, however, lends weight to the argument that the trend towards an increased slope or decreased growth rate is systematic due to the stabilising effect of an increased interfacial magnetic pressure. Furthermore, the magnitude of the trend is consistent with the theoretical calculations.

The dependence of the stable length, l, on the strength of the magnetic field at certain magnetic fluid concentration cannot be seen in Figs. 6–8. This is because it was technically difficult to change the strength of the magnetic field at the interface effectively. When the gap between the magnetic poles was increased from 16 to 20 mm, and finally to 24 mm, the increased magnetic field at the interface of the fluids was within the uncertainty of the Gauss meter. The change of the magnetic field strength was not enough to make the change in the flow observable. To clarify the effect of the magnetic field strength at the interface, further investigations are needed.

In the present case, however, where the trend is hidden within the experimental uncertainty, it is possible to combine the results for all experiments into a single expression. Then the expression for the stable length becomes

$$l = (v - v_0)\frac{\ln(A_m/\eta_1)}{\gamma} = (v - 0.147\,\mathrm{m\,s^{-1}}) \times 0.267\,\mathrm{s}, \tag{8}$$

where the values for the minimum velocity, $v_0 = 0.147$ m s^{-1}, the growth rate, $\gamma = 79$ s^{-1}, and the amplification factor, $\ln(A_m/\eta_1) = 21$, are the average values for the three cases listed in Table 2.

The maximum attainable stable length for the experiments was limited to about 70 mm, compared to a geometrical maximum limit of 160 mm. It was observed that the maximum stable length or maximum velocity obtained increased with the increase in magnetic fluid concentration. The maximum of the stable length and velocity increased from 45 mm and $v = 0.31$ m s^{-1} at a concentration of 0.5% to 57 mm at $v = 0.36$ m s^{-1} and a concentration of 1.0%. At through-flow velocities larger than this maximum, magnetic fluid was flushed out through the outlet by the stream of water. The observations indicate that a distinct change in the flow type occurred, presumably due to a different instability not considered here. The systematic increase in the stable length with ferrofluid concentration suggests that an increased magnetic pressure acting on the interface stabilised the liquid column with respect to this instability.

Figures 9 and 10 are results of the most unstable wavelength, $\lambda = 2\pi r_0/k^*$, depending on magnetic Bond number when the inlet diameter, d, is 1.7 and 2.2 mm, respectively. The vertical axis is the wavelength and the horizontal axis is the magnetic Bond number. The solid lines are theoretical results as calculated by using the dimensionless wave number in Fig. 1 and the

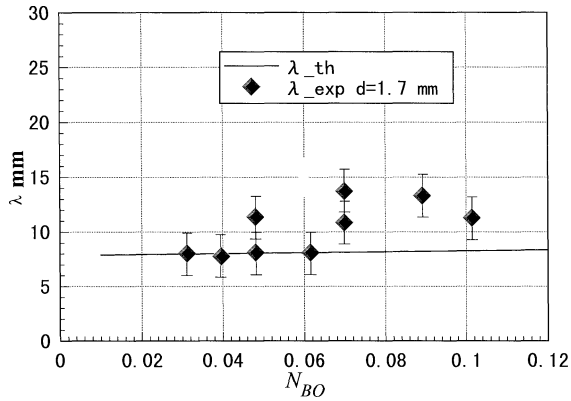

Fig. 9. Unstable wavelength against magnetic Bond number ($r_0 = 0.85$ mm).

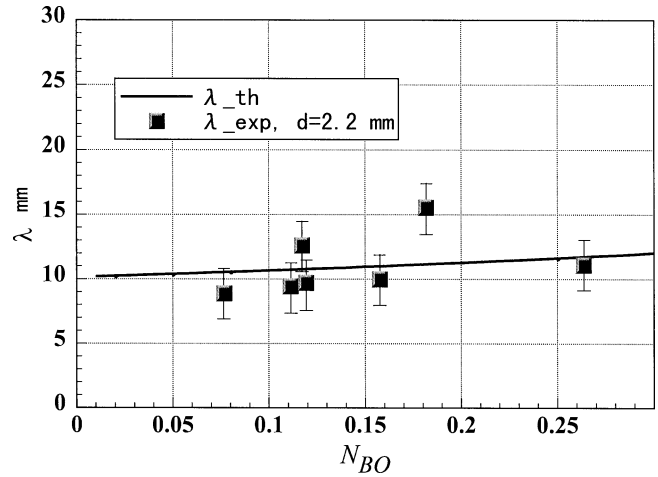

Fig. 10. Unstable wavelength against magnetic Bond number ($r_0 = 1.1$ mm).

marked points are experimental results. The wavelength λ was obtained on a computer screen by measuring the distance between two adjacent highest points of a wave on a photograph taken in experiments. The locations of the highest points of the wave was estimated by human eyes, in which the uncertainty could be as large as ±2 mm. Because the magnetic fluid is opaque, it was very difficult to judge at which point the column began to break up. Drag and buoyancy might both affect the observed wavelength at large amplitudes, as they act stronger on the expanded part of the wavy column than on the contracted phase. Since both act in the direction opposing the flow, one could expect the measured wavelength to be shorter than the expected wavelength. It is therefore more precise to measure the wavelength as soon as the unstable wave can be seen. The uncertainty of the magnetic Bond number, N_{BO}, is governed by the uncertainties of the water column radius, magnetic susceptibility, magnetic field and the interfacial tension, and it was about ±20% in the present experiments.

In Fig. 9, the uncertainty ranges of four experimental points, all for relatively small magnetic Bond numbers, are consistent with the theoretical line, whereas towards larger values of N_{BO}, the observed waves tend to have a larger wavelength than expected. In Fig. 10, almost all experimental results are consistent with the theoretical line. A good agreement with the theoretical results can be seen under different water column radii.

5. Conclusions

Unstable interfacial waves between a magnetic fluid and a diamagnetic fluid column have been studied in the present paper. The results show that the linear solution can predict the onset and characteristics of the growing wave reasonably well. The stability condition of a diamagnetic liquid column kept in a magnetic fluid by a non-uniform magnetic field, whose strength can be expressed as $H = H_a f(r)$, is $r_0 f'(r_0) f(r_0) N_{\mathrm{BO}} \geqslant 1$. At $r_0 f'(r_0) f(r_0) N_{\mathrm{BO}} < 1$, the column is unstable when the

wavelength of the disturbance is shorter than $(2\pi r_0)/\sqrt{1 - r_0 f'(r_0) f(r_0) N_{\mathrm{BO}}}$. Because disturbances usually consist of all wavelengths, the liquid column is not stable when the magnetic Bond number fulfils $r_0 f'(r_0) f(r_0) N_{\mathrm{BO}} < 1$ but a finite length of a stable fluid column can be obtained when the fluid flow rate is higher than critical value. For liquid columns kept in free space, Eq. (3) suggests that, to maintain a stable column, the liquid has to be diamagnetic.

References

[1] J.R. Gao, B.B. Wei, Containerless solidification of undercooled NdFeZrB alloy droplets in a drop tube, J. Alloys Compd. 285 (1999) 229–232.
[2] S.K. Chung, E.H. Trinh, Containerless protein crystal growth in rotating levitated drops, J. Cryst. Growth 194 (1998) 384–397.
[3] W.K. Rhim, K. Ohsaka, P.F. Paradis, R.E. Spjut, Noncontact technique for measuring surface-tension and viscosity of molten materials using high-temperature electrostatic levitation, Rev. Sci. Instrum. 70 (1999) 2796–2801.
[4] B. Lorber, R. Giege, Containerless protein crystallization in floating drops – application to crystal-growth monitoring under reduced nucleation conditions, J. Cryst. Growth 168 (1996) 204–215.
[5] K. Nagashio, Y. Takamura, K. Kuribayashi, Y. Shiohara, Microstructural control of Ndba3Cu307 – delta superconducting oxide from highly undercooled melt by containerless processing, J. Cryst. Growth 200 (1999) 118–125.
[6] M. Lane, K.T. Forest, E.A. Lyons, B.D. Bavister, Live births following vitrification of hamster embryos using a novel containerless technique, Theriogenology 51 (1999) 167.
[7] E. Beaugnon, R. Toumier, Levitation of organic materials, Nature 349 (1991) 470.
[8] M.P. Mahajan, P.L. Taylor, C. Rosenblatt, Magnetic levitation of liquid-crystals, Liq. Cryst. 23 (1997) 547–550.
[9] M.A. Weilert, D.L. Whitaker, H.J. Maris, G.M. Seidel, Magnetic levitation of liquid-helium, J. Low Temp. Phys. 106 (1997) 101–131.
[10] T. Aoyama, Y. Takamura, K. Kuribayashi, Containerless solidification of Si–Ge binary alloy by means of laser-heating electromagnetic-levitation, Jpn. J. Appl. Phys. 37 (1998) L687–L690.
[11] Japanese Society of Steel, Electromagnetic Processing of Materials, Tohoku University Press, October 1998.
[12] A.J. Rulison, J.L. Watkins, B. Zambrano, Electrostatic containerless processing system, Rev. Sci. Instrum. 68 (1997) 2856–2863.
[13] E.G. Lierke, Acoustic levitation – a comprehensive survey of principles and applications summary, Acustica 82 (1996) 220–237.
[14] J.K.R. Weber, D.S. Hampton, D.R. Merkley, C.A. Rey, M.M. Zatarski, P.C. Nordine, Aeroacoustic levitation – a method for containerless liquid-phase processing at high temperatures, Rev. Sci. Instrum. 65 (1994) 456–465.
[15] R.J. Bayuzick, N.D. Evans, W.H. Hofmeister, M.B. Robinson, Microgravity containerless processing in long drop tubes, in: NASA Conference Publication, 1984, pp. 243–259.
[16] A.S. Gandhi, A. Saravanan, V. Jayaram, Containerless processing of ceramics by aerodynamic levitation, Materials Science & Engineering A: Structural Materials: Properties, Microstructure and Processing 221 (1996) 68–75.
[17] M.A. Weilert, D.L. Whitaker, H.J. Maris, G.M. Seidel, Laser levitation of superfluid helium, J. Low Temp. Phys. 98 (1995) 17–35.
[18] M.V. Berry, A.K. Geim, Of flying frogs and levitrons, Eur. J. Phys. 18 (1997) 307–313.
[19] N.I. Wakayama, Magnetic buoyancy force acting on bubbles in nonconducting and diamagnetic fluids under microgravity, J. Appl. Phys. 81 (1997) 2981–2984.
[20] S. Ueno, M. Iwasaka, Properties of diamagnetic fluid in high-gradient magnetic-fields, J. Appl. Phys. 75 (1994) 7177–7179.
[21] M. Fujisaki, S. Naito, K. Yamaguchi, M.K. Park, S. Oshima, M. Nakagawa, R. Yamane, Levitation of diamagnetic liquid droplet by means of magnetic force, in: The 8th Symp. on Electric and Magnetic Related Dynamics, Tokyo, 1996, pp. 373–379, (in Japanese).
[22] J. Mai, R. Kobayashi, M. Nakagawa, S. Oshima, R. Yamane, Axial oscillation of a magnetically levitated non-magnetic fluid column inside a straight magnetic pipe, Fluid Dyn. Res. 24 (1999) 147–159.
[23] J. Mai, A. Shoda, M. Nakagawa, S. Oshima, R. Yamane, Stability of a magnetically levitated diamagnetic fluid column, JSME Int. J. B-Fluid T. 42 (1999) 533–560.